Respiratory Medicine (2012) **106**, 127–137

Available online at www.sciencedirect.com

SciVerse ScienceDirect

journal homepage: www.elsevier.com/locate/rmed

Imaging parenchymal lung diseases with confocal endomicroscopy

Richard C. Newton [a,b,*], Samuel V. Kemp [c], Guang-Zhong Yang [a], Daniel S. Elson [a], Ara Darzi [b], Pallav L. Shah [c]

[a] *Hamlyn Institute for Robotic Surgery, Imperial College, London SW7 2AZ, United Kingdom*
[b] *Department of Surgery and Cancer, St Mary's Hospital, Imperial College, London W2 1NY, United Kingdom*
[c] *Department of Respiratory Medicine, Royal Brompton Hospital, Fulham Road, London SW3 6NP, United Kingdom*

Received 25 July 2011; accepted 24 September 2011
Available online 14 October 2011

KEYWORDS
Probe based confocal endomicroscopy;
Optical biopsy;
Parenchymal lung disease;
Diffuse lung disease;
Emphysema;
Fluorescein

Summary
Background: "Optical biopsy" using bronchoscopic probe-based confocal endomicrosocopy (pCLE) provides real time images of the autofluorescent elastin scaffold of the healthy acinus.
Objectives: To establish how different parenchymal lung diseases (PLDs) alter the pCLE image, if intravenous fluorescein provides additional diagnostic information, and to assess pCLE's safety for investigating PLDs (UK REC: 09/H0708/18).
Methods: 116 bronchopulmonary segments were examined in 38 patients and 4 healthy non-smoker volunteers. pCLE images were correlated with consensus multidisciplinary diagnosis from HRCT, bronchoalveolar lavage, and transbronchial/CT guided biopsies.
Results: Severe emphysema is evident on pCLE imaging, with increased spacing between septal walls, sudden loss of fluorescence from bullae and a subsequent reticular pleural image. Other PLDs demonstrated marked loss of lobular autofluorescence and distinctiveness. In all diseases imaged, differentiation between septal wall and microvessel elastin is more difficult in diseased versus healthy acini. Smokers displayed a hyperfluorescent 15-30 micron cellular alveolar infiltrate - alveolar macrophages on *in vitro* BAL analysis. Varied intravenous fluorescein doses only create a hyperfluorescent foreground with bubbles. pCLE can cause pleuritic discomfort but there were no pneumothoraces. 3 patients had transient bleeding, and *in vivo* tearing of septal walls and microvessels abutting the probe was observed.
Conclusions: Marked emphysema is demonstrable from loss of elastic walls. The detail of high-resolution pCLE images is attenuated in other PLDs without further clarity from intravenous fluorescein. Nevertheless, pCLE is safe for PLD investigation. These findings form a basis

* Corresponding author. Hamlyn Institute for Robotic Surgery, Bessemer Building, Imperial College London, South Kensington Campus, London, SW7 2AZ, United Kingdom. Tel.: +44 7980005675; fax: +44 02075945196.
E-mail addresses: richardnewton22@yahoo.co.uk (R.C. Newton), pallav.shah@imperial.ac.uk (P.L. Shah).

0954-6111/$ - see front matter
doi:10.1016/j.rmed.2011.09.009

for future work to harness pCLE's potential utility as part of a multiassessment modality for PLD diagnosis.

Introduction

To accurately diagnose many parenchumal lung diseases (PLDs) or solitary peripheral nodules, a multidisciplinary assessment is required.[1] This combines information from the clinical presentation, interpretation of the high-resolution computed tomography (HRCT) images, and microbiological, cytological, and histopathological clues provided by bronchoscopy. Histopathological analysis has the greatest influence upon establishing a diagnosis,[2] but it does not always provide a definitive answer[3] and is not free from risk. Indeed, a blind transbronchial biopsy (TBB) carries a 1–12% risk of pneumothorax,[4–7] and a 2–9% risk of bleeding.[5,8,9] For lesions that are inaccessible to TBB, the risks of percutaneous or video assisted thoracoscopic biopsies are greater.[3,10]

Autofluorescence imaging,[11] narrow band imaging,[12] and optical coherence tomography[13] are some of the encouraging biophotonic techniques that are being studied as adjuncts to white-light bronchoscopic imaging and tissue biopsy, but their size prohibits deployment beyond the larger airways. Even the thinnest bronchoscope has a diameter of 2.7 mm.[14] However, recent miniaturisation of the confocal microscope has provided a means of acquiring 3.5 μm resolution images of the upper airways[15–17] and also the acini[18,19] *in vivo*. With probe-based confocal endomicroscopy (pCLE) of the peripheral lung, a stiff 1.4 mm diameter probe is inserted through the biopsy channel of a standard bronchoscope into the alveolar duct; it transmits 488 nm blue argon laser light via 30,000 optical fibres. The probe then detects the fluorescent elastin scaffold of the acinus, and a real time image of the arching elastic fibres forming the backbone of alveoli and blood microvessels is provided on screen. If adjacent images can be readily tracked during steady probe translation, the field of view (FOV) can, in theory, be increased using the device's "mosaicing" software.[20] In current smokers, the image also displays highly fluorescent mobile macrophages. An initial *in vivo* study in 41 healthy subjects has found pCLE to be safe, and has enabled the basic morphology of the resolved structures to be described.[19]

Aims and objectives

This hypothesis-generating prospective observational study was designed to explore a potential role for pCLE in investigating different PLDs. The first aim was to evaluate its ability to detect morphological changes evident in specific diseases. In the brief history of endoscopic pCLE, the gastrointestinal mucosa has been the major organ target.[20] Here, unlike in the elastin rich lung, exogenous fluorescent contrast agents such as intravenous fluorescein or topical acriflavine are required to delineate the cellular architecture of the glands embedded within the epithelium, and demonstrate dynamic *in vivo* blood flow.[21,22] Therefore, the second aim was to establish if intravenous fluorescein provided additional *in vivo* information in pCLE imaging of peripheral lung in health and disease (such as improved delineation of vasculature). The third and final aim was to assess the safety of pCLE in PLD patients. The results from the first 17 subjects have been previously reported in the form of an abstract.[23]

Materials and methods

Subjects

We performed pCLE in 1) healthy non-smoker volunteers, 2) patients with chronic obstructive pulmonary disease (COPD), and 3) patients with other diverse PLDs during their diagnostic bronchoscopy. The healthy subjects had no significant cardiorespiratory disease or bleeding diathesis. All COPD and other PLD patients had HRCT scans performed prior to bronchoscopy. Emphysema severity on HRCT was graded 1-4.[24] All subjects gave prior written informed consent. The study was approved by the Brompton, Harefield & NHLI Research Ethics Committee (09/H0708/18).

Bronchoscopy

Subjects had topical local anaesthesia applied and were given conscious sedation if required (1–5 mg midazolam). They were given 2 L/min oxygen via nasal prongs and monitored with pulse oxymetry. The pCLE laser unit and probes were standard and commercially available (Cellvizio®-Lung, Mauna Kea Technologies, France) producing a 600 μm diameter FOV at 12 frames per second, at an imaging plane depth of up to 50 μm. Subjects were reclined at 45°. The laser unit was warmed up for 15 min before recalibration, and the auto-power setting used. An Olympus 1T260 bronchoscope was used to evaluate the central airways and then advanced into the most distally accessible bronchi, whereupon the probe was gently advanced beyond the distal opening of the working channel until recognisable images were obtained of the acinus. During normal respiration, successive pCLE video loops were acquired of up to six bronchopulmonary segments (BPSs) named according to international nomenclature.[25] In each PLD patient, an attempt was made to optically biopsy contrasting BPSs, displaying both maximal and minimal radiological signs of disease. Where clinically indicated, bronchoalveolar lavage (BAL) was performed using 100 mls of 0.9% saline, and TBB was performed with Olympus EndoJaw disposable biopsy forceps (Model FB-211D). Diagnosis in two patients required subsequent CT-guided percutaneous biopsy. All patients undergoing transbronchial biopsies had post-procedure erect chest radiographs performed.

For the first 5 patients who underwent BAL/TBB correlation, an extended working channel (outer sheath) was initially deployed through the working channel and blindly wedged distally to improve the likelihood that pCLE, BAL and TBB were all obtained from the same location.

During continuous pCLE video acquisition at the end of five bronchoscopies, incremental doses of intravenous 1% fluorescein (Martindales, UK) were injected through a peripheral cannula. A saline flush and a 90 s interval of continuous imaging separated all boluses. A total of 20 mls was administered into the first subject (healthy volunteer) in 5 mls boluses; a final dose which approaches that used in gastroenterological pCLE. The subsequent 4 subjects (2 healthy volunteers and 2 with emphysema) had substantially smaller incremental doses of 0.1 ml, 0.25 ml, 0.4 ml and 1 ml.

BAL/TBB analysis and definitive diagnosis

Differential cell separation, cytopathological examination, and microbiological culture were performed on all BAL fluid samples. Where there was spare BAL fluid, constituent cells were differentially separated, resuspended, and ex *vivo* pCLE imaging performed. TBB samples were fixed in formalin, embedded in wax and 5 μm sections were examined by an expert pathologist. In accordance with current guidelines,[1] all available data was discussed at a multidisciplinary team meeting to reach a diagnostic consensus.

pCLE image acquisition, processing and interpretation

pCLE video loops were recorded in each BPS until a consistent image had been obtained. At least five representative stills were created for each video, for subsequent qualitative appraisal by two observers (RN & PS) using Cellvizio Viewer® software (Mauna Kea technologies, France), including an assessment of the septal walls and vessels (autofluorescence intensity, regularity of structure) and any fluorescent cellular infiltrate. The Cellvizio Viewer® software's mosaicing function was used to create automated mosaics. For each video sequence that enabled mosaic construction, the longest individual mosaic axis was recorded as a quantification of how well the FOV could be retrospectively increased. SPSS was used for statistical analysis.

Results

Subjects

Bronchoscopic pCLE videos and still images were obtained from 4 control volunteers and 1 lung-disease free patient (normal HRCT but cutaneous erythema nodosum) (mean age 34.8 ± 9.7) (Fig. 1A–C), together with 38 patients (mean age 54.9 ± 11.8). BAL, TBB and CT guided biopsy were performed in 23, 21 and 2 patients respectively. Of the TBBs, 2/21 (9.5%) yielded no alveolar parenchyma, 4/21 (19%) provided pathognomic features, another 7/21 (33.3%) provided essential information for the diagnosis, and the remaining 8/21 (38%) were non-specific. Final diagnoses were COPD (13 patients mean age 61.7 ± 6.8), or other PLD (24 patients mean age 48.9 ± 13.6) (Table 1). The only two current smokers were PLD patients (sarcoid and respiratory bronchiolitis). The single chronic bronchitis patient had smoked until 2 weeks before bronchoscopy. RB1 and LB1/2 were the only BPSs that were not always possible to cannulate, but this occurred only during 4 bronchoscopies. Previously, cannulation of these BPSs has been regarded as

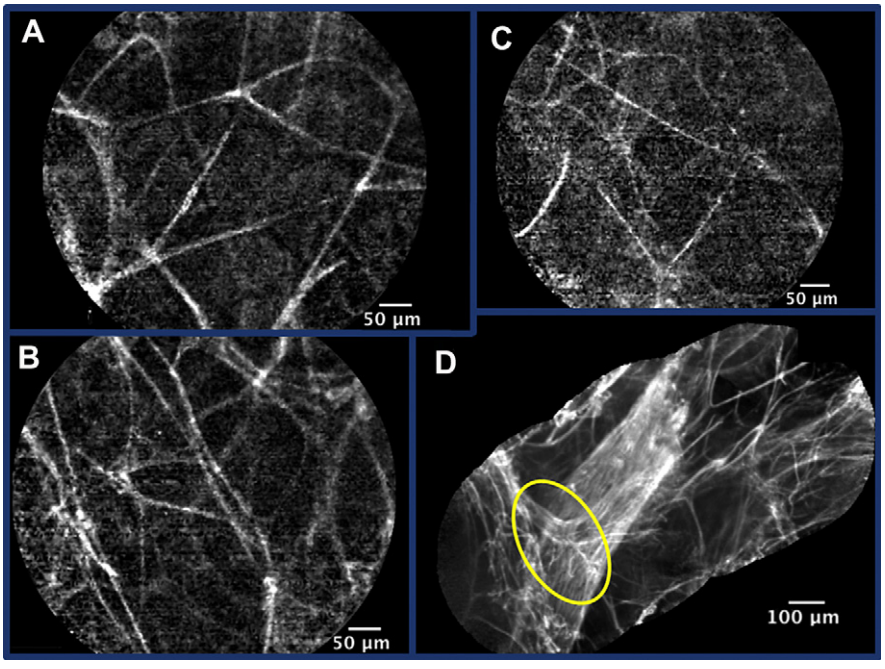

Figure 1 Still pCLE images in A,B & C are from healthy BPSs and show fine undistorted septal wall elastin architecture (<10 μm thickness). Age seems to play a role in the septal wall fluorescence intensity (A and B are from a 52 year old patient; C was aged 29). Mosaicing was able to increase the FOV in 65/116 BPSs: D shows the longest mosaic created (1268 μm); the oval highlights a 150 μm microvessel with a small branch (from a BPS with grade 1 emphysema).

Table 1 The main diagnoses of the 42 subjects bronchoscoped, providing the 116 BPSs that were imaged.

	Number of subjects (main diagnosis)	Overall number of affected BPSs imaged
Healthy		
Volunteers	4	19
Nil abnormal on CT, TBB & BAL, or remote from diseased area	1	8
Subtotal	*5*	*27*
COPD		
Grade 1 emphysema	2	2
Grade 1 emphysema with partial collapse	1	1
Grade 2 emphysema	0	3
Grade 2 emphysema with mild infection	0	1
Grade 3 emphysema	0	3
Grade 3 emphysema with mild infection	1	1
Grade 4 emphysema	8	15
Chronic bronchitis	1	3
Subtotal	*13*	*29*
Other parenchymal lung diseases		
Respiratory bronchiolitis	1	5
Pulmonary sarcoidosis	4	12
Mild radiotherapy damage	1	1
Tuberculosis	1	4
Pulmonary fibrosis with infection	1	1
Drug-induced pneumonitis	2	3
Peri-chemotherapy pneumonia	7	19
Amyloidosis	1	2
Peripheral non small cell lung cancer	1	1
Bronchioloalveolar carcinoma	1	5
Metastatic cancer (breast, endometrial or fibrosarcoma)	4	7
Subtotal	*24*	*60*
Total	42	116

impossible owing to probe stiffness.[19] Each subject had 1-6 BPSs optically biopsied creating 116 pCLE videos for analysis. The extended working channel was used for the first 5 subjects, but following concern that it was slightly impeding the action of the TBB forceps and the fluid flow for the BAL, it was abandoned.

pCLE images of emphysema

It is evident from studying the 116 video loops and representative stills, that the appearance of copious, regular, 10 μm elastic fibres within the alveolar septal wall structure previously described in healthy subjects,[19] and illustrated in Fig. 2, becomes variably disorganised in all peripheral diseases (Table 2). For example, pCLE highlights some of the morphological alterations in severe emphysema, the main one being a loss of the number of septal walls (Fig. 2). In many cases there is distortion of the remaining emphysematous septal walls, or thickening that leads to an inability to distinguish septal wall from microvessel (Figs. 2c and 4). In 2 emphysematous BPSs containing large bullae, a sudden black image was followed by a fine reticular pattern, suggesting the possibility that the inner surface of the visceral pleura had been reached via a bulla (Fig. 2E and F).

pCLE images of other PLDs

In most parenchymal lung diseases other than emphysema, the pCLE architecture becomes unrecognisable (Figs. 3 and 4f). The autofluorescence is substantially reduced and the images become indistinct and noisy. The most radiologically affected areas tend to display the most disruption and loss of autofluoresence in their corresponding pCLE images. This contrasts with BPSs exclusively affected by emphysema which, as described, have a smaller number of septal walls per FOV, creating the appearance of "holes", but they do not appear to lose autofluorescence intensity, and the elastin scaffold of the acinus tends to retain its distinctiveness even in severe disease, even if sometimes vessels become indistinguishable from septal wall.

Whilst the septal wall structure was more distinct in healthy volunteers than in subjects with marked disease, the autofluorescence was generally weaker than healthy or emphysematous areas of older patients. This effect of age on autofluorescence has previously been described.[19]

Inflammatory cells

The appearance of undetermined 3 μm specks (particularly on approach to the acinus), mucus globules/bubbles or even faint inflammatory cells is a non-specific finding to healthy and diseased areas (Fig. 5). However, brightly autofluorescing 15–30 μm cellular infiltrates were exclusively observed in the BPSs of the only 2 current smokers in the study (respiratory bronchiolitis and sarcoid), as well as one recently ex-smoker with chronic bronchitis. The 3 other sarcoidosis patients were non smokers and their *in vivo* pCLE and *ex vivo* BAL pCLE images had no visible inflammatory cell infiltrate. Differential cell separation of the 2 current smokers' BAL fluid demonstrated that the responsible cells were autofluorescent macrophages. The subject with chronic bronchitis had endobronchial washings only, which displayed no *ex vivo* fluorescent cells.

Mosaic function

The automated mosaic function was used on the Cellvizio Viewer®software. Mosaics were creatable for 65/116 video loops, but the mean maximum mosaic length was a modest 757 ± 125 μm. Video loops with bright distinct images, where there was some controlled movement of the probe tip tended to yield longer mosaics (Fig. 1D).

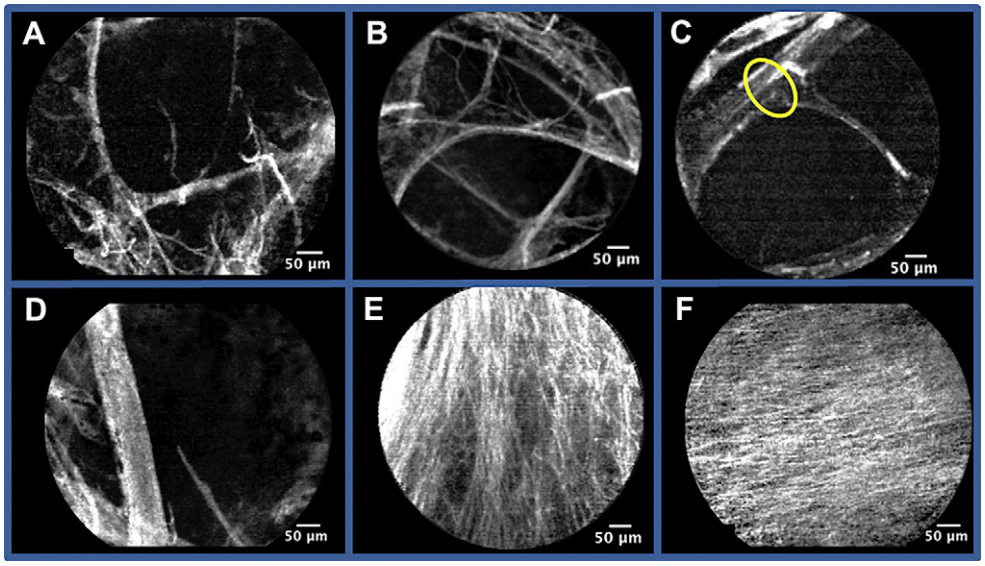

Figure 2 The number of visible septal walls tends to reduce as emphysema worsens: grade 1 emphysema (A), grade 4 (B). C and D are images near large bullae. The ellipse in C highlights arching fibres that probably represent distorted and thickened septal wall, though using discrimination by thickness they could alternatively be microvessel. D shows a probable vessel but minimal septal wall. E and F are images of pleura beyond bullae.

Intravenous fluorescein

With intravenous fluorescein 1%, 0.25 mls was the minimum required to observe a change. This change consists of a hyperfluorescent foreground containing non-fluorescent bubbles; it appears within a few seconds of drug administration and is not initially confined to the microvessels (as might be expected) (Fig. 6). Therefore, there is no discernible increase in the autofluoresence of the septal walls, microvessels or cells during incremental administration of the drug.

Safety and acceptability

To acquire adequate pCLE footage for subsequent analysis, each BPS imaged added a mean of 112 ± 48.9 s to the bronchoscopy procedure (prior to any fluorescein based imaging). During or after pCLE, prior to TBB, blood originating distal to the bronchoscope tip, along the path of the probe towards the acinus, impaired the bronchoscopic view in 3 patients by seeping proximally into the subsegmental bronchus. However, all bleeding was minimal and spontaneously resolved without further complication or need for

Table 2 A summary of the observations and measurements from the 116 BPSs analysed. Whilst the elastin scaffold morphology with emphysema is most likely to appear distorted, structures tend to be vivid and brightly autofluorescent. Diminution of both autofluorescence and recognisable distinct structure is common in other PLDs (ANOVA was used for mosaic length, and 2-sided chi-square tests for the other observations).

Observation	Healthy/Normal ($N = 27$)	COPD ($N = 29$)	Other PLD ($N = 60$)
Decreased autofluorescence of individual elastic structures ($p = 0.002$)	12/27 = 44.4%	1/29 = 3.4%	19/60 = 31.7%
Unrecognisable structure & decreased distinctiveness ($p = 0.000000056$)	7/27 = 25.9%	5/29 = 17.2%	45/60 = 75%
Distorted septal wall morphology ($p = 0.000000097$)	1/27 = 3.7%	22/29 = 75.9%	35/60 = 58.3%
Snapped septal walls or vessels ($p = 0.00019$)	2/27 = 7.4%	15/29 = 51.7%	11/60 = 18.3%
Autofluorescent macrophages (15–30 μm & mobile) ($p = 0.075$)	0/27 = 0%	3/29 = 10.3%[b]	10/60 = 16.7%[a]
Mucus globules/bubbles ($p = 0.935$)	9/27 = 33.3%	11/29 = 37.9%	21/60 = 35%
3 μm specks ($p = 0.108$)	6/27 = 22.2%	8/29 = 27.6%	26/60 = 43.3%
Are mosaics creatable? ($p = 0.0000091$)	7/27 = 25.9%	26/29 = 89.7%	32/60 = 53.3%
Mean maximum mosaic length (μm) ($p = 0.00042$)	691 ± 84.9	829 ± 148	714 ± 78.4

[a] The few BPSs displaying autofluorescent macrophages were from the only two current smokers in the study, both with other PLDs.
[b] A COPD patient who had only quit smoking 2 weeks previously.

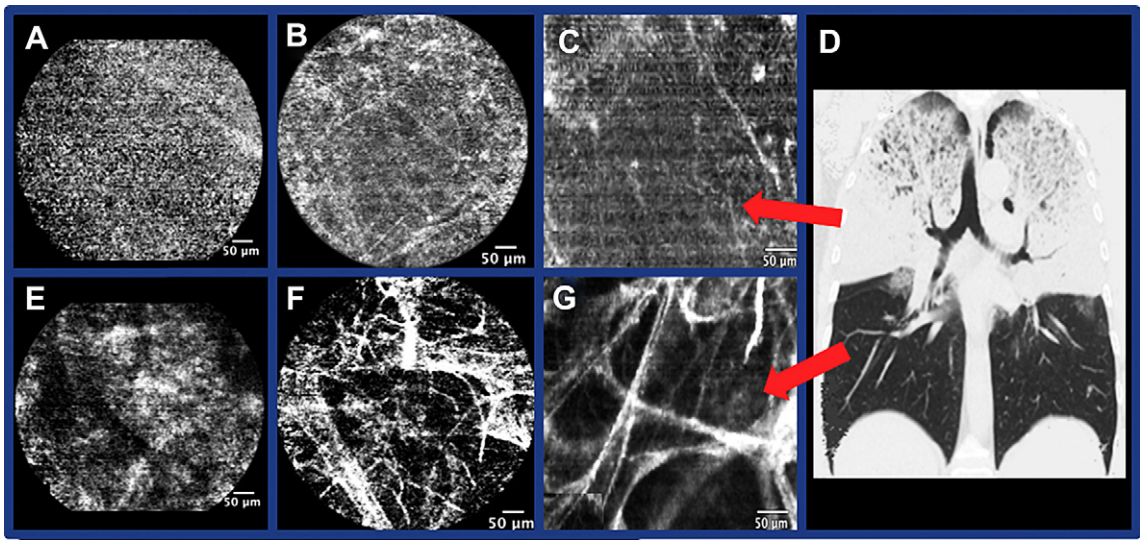

Figure 3 Many PLDs cause a non-specific loss of fluorescence and distinctiveness. This is demonstrated with a peripheral metastatic fibrosarcoma deposit (A), an organising pneumonia (B), and an area of lung affected by a lymphocytic infiltration secondary to a peri-chemotherapy pneumonia (F). In a patient with bronchioloalveolar carcinoma, HRCT showed severely affected upper lobes (D), and pCLE provided virtually no recognisable autofluorescence within the right upper lobe (C) whereas the spared right lower lobe showed distinct alveolar structures with greater autofluorescence (G). E was acquired from maximal distal cannulation of LB6 in a patient with tracheobronchial amyloidosis: the "cotton wool like" autofluorescence was similar to that observed in pCLE of endobronchial amyloid deposits.[26]

intervention. Of note, one of these patients had a clotting abnormality (prothrombin time of 19 s), and within the probed BPS of another patient was a metastatic breast tumour displaying microvessel invasion. Nevertheless, there was clear observation of a microvessel being snapped *in vivo* by the probe in three separate BPSs (Fig. 7E, *see online supplement for videos*). The probe sometimes causes pleuritic pain during image acquisition, but there were

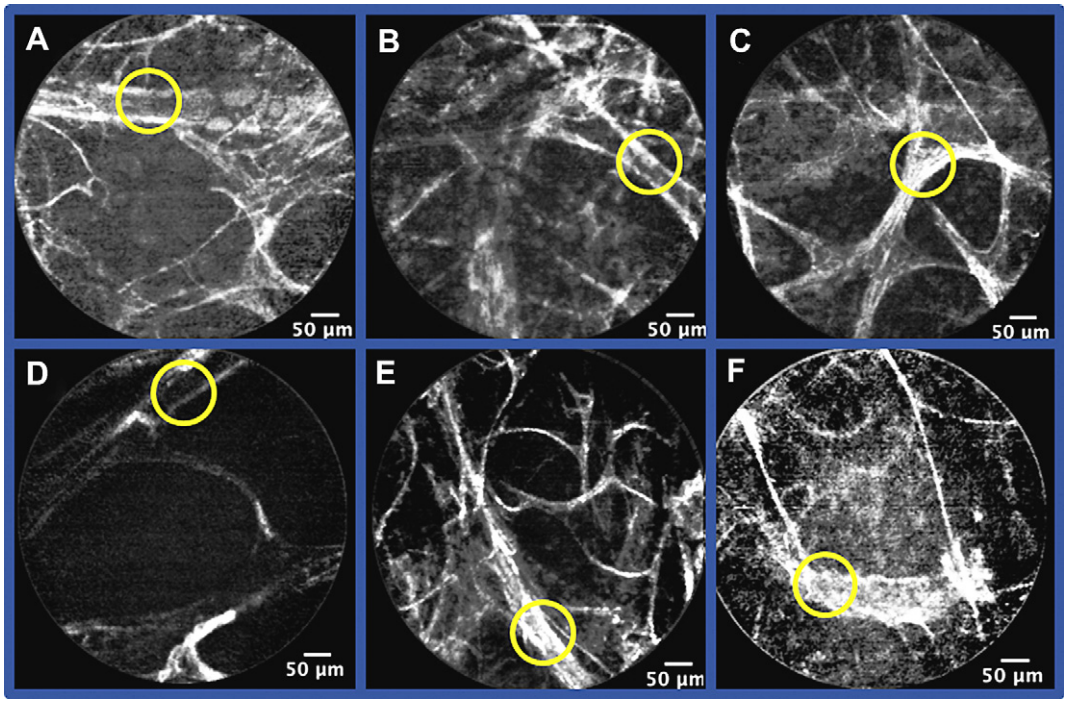

Figure 4 In health, differentiation between microvessels and septal walls (Fig. 1) is done on diameter and shape characteristics.[19] This is not as straightforward in diseased BPSs, and here the circles show indeterminate structures from diseased BPSs which cannot be identified as either structure on the basis of their shape or intermediate calibre. A-E are from emphysematous BPSs (grades 2, 3, 3, 4, and 4 respectively) and F is from a BPS with drug-induced pneumonitis.

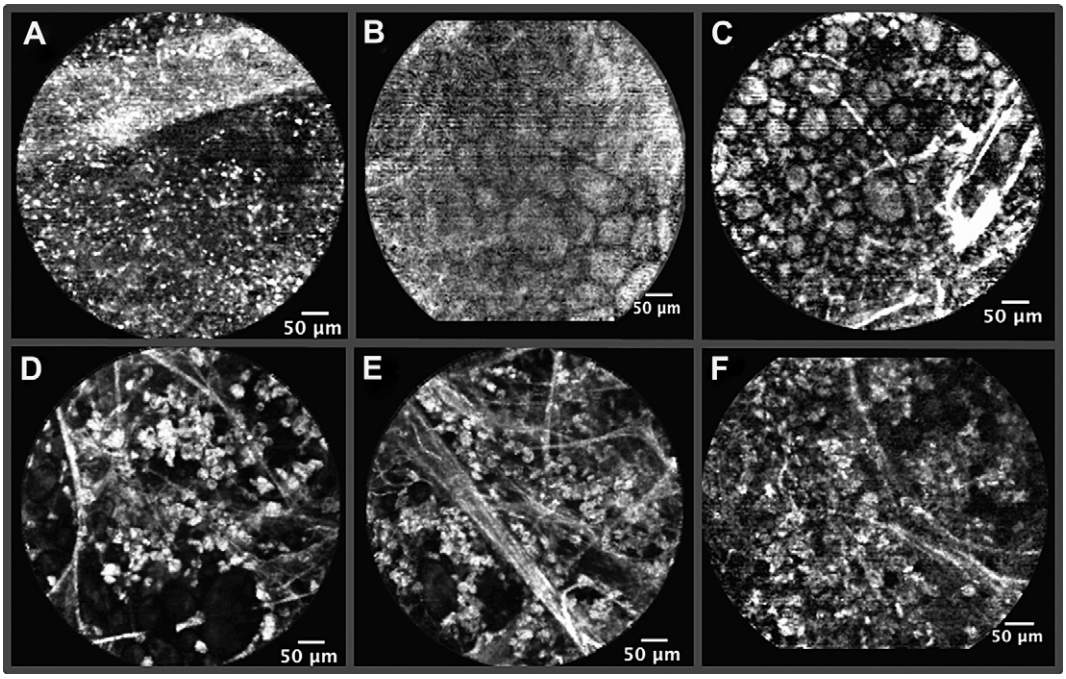

Figure 5 Bright indeterminate 3 μm specks are common on approach to the acinus regardless of smoking status (A is from a patient with pneumonia). Apparent mucus blobs or bubbles are non-specific (B is from a resolving pneumonia, and C is from a BPS with grade 3 emphysema). Whilst some very faint cells are suggested even in non-smokers, brightly autofluorescing alveolar macrophages are exclusive to smokers (or those with a recent smoking history) regardless of disease (D&E are from RB4 and RB6 of a recently quit heavy ex-smoker with chronic bronchitis). F shows that these macrophages sometimes "drown out" the alveolar walls (respiratory bronchiolitis).

no pneumothoraces. The largest fluorescein dose injected caused retching during the procedure in one healthy subject. Seemingly snapped elastic fibres of the septal walls flapped around on the video loops of 28 BPSs (Fig. 7A—D). It is possible that pre-existing disease may create or predispose to this disruption; it was indeed more commonly observed in COPD BPSs than in areas that were affected by other PLDs or healthy lung. Nevertheless, direct damage from the probe was witnessed in 6 BPSs as septal walls snapped during image acquisition (Fig. 7D).

Supplementary video related to this article can be found at doi:10.1016/j.rmed.2011.09.009.

Discussion

A previous study has demonstrated that pCLE accurately displays the morphology of the elastin microskeleton within the healthy acinus,[19] which has led to speculation that pCLE may provide diagnostic clues in peripheral lung diseases.[18,27,28] This study has described the feasibility and findings of pCLE imaging in a group of patients with varied parenchymal diseases.

Regarding image interpretation, the best case scenario was that alterations to elastin would be specific to individual diseases and provide unique image features such that, for example, non-necrotising granulomas were visible in sarcoidosis,[29] and the fibrotic zones of dense collagen found in pulmonary fibrosis were enough to specifically alter the elastin appearance.[30] However, the pathognomonic features of specific diseases, observed under standard haemotoxylin and eosin histopathological microscopy are unlikely to match the changes occurring to the elastin. Nevertheless, elastin structure and production is known to alter in lung disease,[31—34] and the most salient image finding from this series is the degree to which many peripheral diseases (emphysema excluded) are able to create a non-specific attenuation of the stunning highly recognisable images of healthy acini. The observed loss of distinctiveness and autofluorescence in the non-emphysematous diseases within this study may be due to elastin destruction, alveolar collapse or substances such as collagen, blood, inflammatory infiltrate or mucus impeding the incident laser light and emitted autofluorescence.

Predictably,[19] the autofluorescence intensity of individual fibres was greater in the older subjects; the healthy volunteers were young and whilst their individual septal walls were generally distinct, they displayed consistently weaker autofluorescence than from older non-diseased BPSs, or those BPSs only affected by emphysema.

It appears that severe emphysema is often evident on pCLE imaging with dark holes and a reduction in the number of septal walls visible in each frame. Residual elastin is often thickened or disrupted. This is perhaps logical, considering that a major feature of COPD is fragmentation and loss of alveolar elastin.[35] It remains to be established whether these are sufficiently reliable diagnostic findings, and whether milder disease is adequately demonstrable. If so, pCLE could be employed to grade the severity of emphysema for trials, or to assess the efficacy of interventions. Currently, subclinical COPD in asymptomatic smokers is screened for using spirometry[36] but whilst much

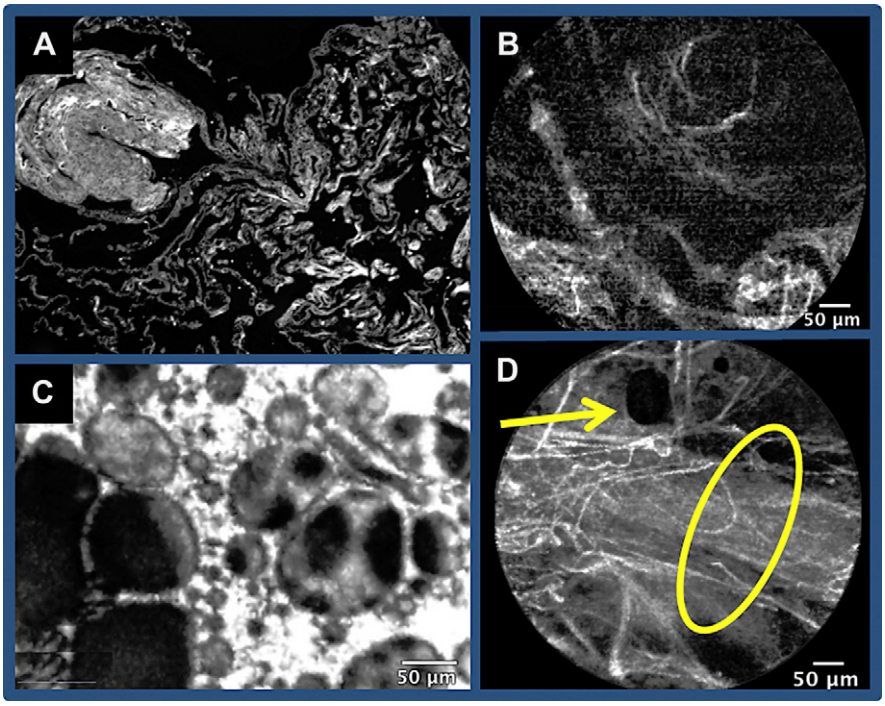

Figure 6 Compared to standard biopsy, there is reduced resolution/diagnostic information with conventional elastin autofluorescence pCLE: from the same sarcoid BPS, compare the H&E stained TBB (autofluorescent microscopy ×200) (A) of a pathognomonic non-necrotising granuloma to the non-specific disruption seen with pCLE (B). The administration of intravenous fluorescein does not provide additional information: it causes a general white appearance of the mucus/surfactant (C shows a healthy BPS following injection of 5 ml of 1%) with bubbles displacing the contrast agent. All other acinar structures are disguised. Even when tiny quantities are used (such as 0.4 ml of 1% in D), the microvessels (marked by the ellipse) are no more distinct, but bubbles are still evident where the newly fluorescing mucus is being disturbed.

more invasive, pCLE could have an additional diagnostic role, particularly if it had greater sensitivity for detecting early morphological damage which was predictive for future symptomatology. However, centrilobular emphysema tends to be heterogeneous which will inevitably create sampling bias; a particular problem in alveolar pCLE where to image a new area, mural restraint of the probe necessitates blind reinsertion into the BPS in the hope of cannulating a different terminal bronchiole. Conversely, the homogeneity of panacinar emphysema in alpha-1-antitrypsin deficiency makes early diagnosis difficult using HRCT; this provides a possible niche for pCLE. In this study, it should also be highlighted that two patients with bullae inadvertently had what is likely to be the first described *in vivo* bronchoscopic imaging of the inner surface of the elastin rich visceral pleura.[37]

Thiberville et al. bronchoscoped 41 healthy volunteers and confidently measured the septal walls as being 10 ± 2.7 μm and the microvessels as 90 ± 50 μm.[19] However, in the diseased BPSs, discrimination between these two image components was often impossible. This is likely due to pathological disruption of the elastin architecture forming the septal walls and microvessels,[38–40] along with in many BPSs, the disease related reduction of image distinctiveness and autofluorescence described.

Using the mosaicing software, the standard 600 μm FOV could only be modestly increased in just over half of the BPSs overall, and only two BPSs yielded mosaics >1 mm. Unlike pCLE in less constrained areas, such as the proximal endobronchium or the gastrointestinal lumen, the probe cannot easily be translated, and within the acinus gentle withdrawal or further advancement does not always provide adjacent images to stitch together. The mosaicing function was likely impaired by fainter septal walls in the younger subjects, and distinct feature loss in non-emphysematous disease.

Whilst this series included only three current or recently quit smokers, the previous finding in healthy subjects that bright autofluorescent macrophages are specific to smokers or ex-smokers,[19] seems to remain true in disease. Whilst there was a suggestion of similarly sized faint cells in the acinae of several subjects, the inflammatory cells in the video loops from the current and recently quit smokers were very bright and clearly independently mobile and therefore distinct from the septal walls they were within. The smokers' BAL fluid uniquely demonstrated fluorescent cells (macrophages). The fluorescence imparted upon alveolar macrophages from cigarette smoking takes years to fully diminish[41] and there is *in vitro* evidence that air pollutants have a similar effect on macrophage fluorescence.[42] These factors could explain any less obvious fluorescent cellular infiltrates. Further work is needed to elucidate the identity of the mucus globules/bubbles and the bright 3 μm specks.

The prediction of probe destination remains an issue. Even in Thiberville et al's healthy cohort, over 10% of cannulated BPSs failed to provide an alveolar image,[19] presumably because of an inability to adequately deploy

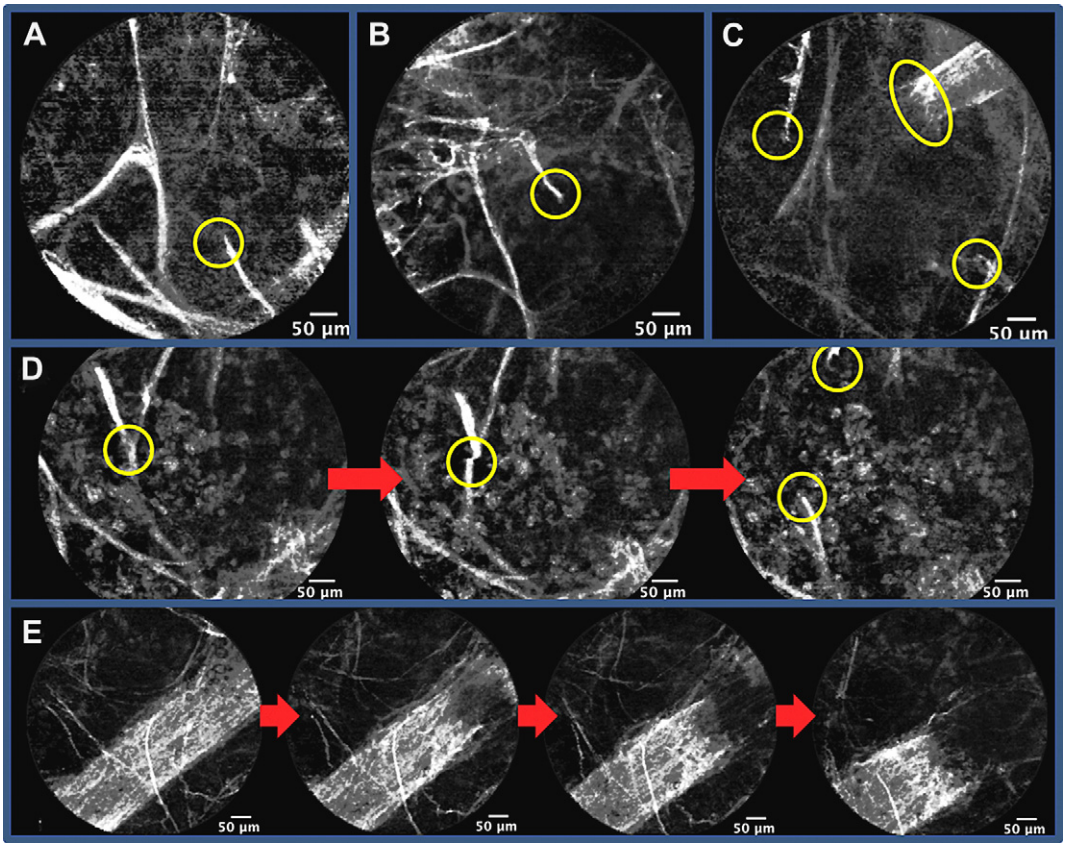

Figure 7 Free ends of septal walls, observed on video loops to flutter loosely, were apparent in 28/116 BPSs (highlighted with circles in A, B, C and D). This phenomenon could be partly illustrative of the primary disease, however, in 6 BPSs, individual septal walls were observed to fracture, separate and then their blind ends swing freely, presumably from the axial pressure of the probe (demonstrated in C, and in D across 3 sequential frames; each separated by 83 ms). Microvessels were also observed to snap under axial pressure in 4 BPSs (highlighted by an oval in C, and sequential frames shown in E). A is from a grade 1 emphysema BPS, B, C and E are from different grade 3 and 4 BPSs, and D is from a patient with respiratory bronchiolitis (*see online supplement for videos*).

or position the probe beyond the respiratory bronchiole. In severely diseased BPSs it was difficult to ascertain if a reduction in image quality represented this incomplete deployment, or if the probe was imaging a bulla/diseased area. Similarly, it is not possible to confirm that the pCLE image was taken from exactly the same location as the diagnostic TBB and BAL. Whilst the TBB forceps and pCLE probe both follow the path of least resistance, and are of similar diameter and stiffness, they were blindly deployed into the subsegmental bronchus. Whilst the possibility of multiple potential terminal destinations of the pCLE probe and TBB forceps is of minimal consequence in BPSs affected by diffuse homogeneous disease, focal or patchy disease may cause difficulty with reliable correlation, justifying fluoroscopic guidance. In this study, an extended working channel was trialled but abandoned owing to ergonomic concerns during BAL and TBB.

Intravenous fluorescein is the *modus operandi* for pCLE in the GI tract by highlighting the calibre, course and leakage of microvessels,[43] as well as providing fluorescence of the epithelium and glands. For this study, it was postulated that intravenous fluorescein might facilitate the discrimination between microvessels and septal walls, and therefore might have a role in diagnosis. However, there was no concentration that provided a useful role in peripheral lung pCLE imaging as there is "white-out" of the image before delineation of any microvessels can take place. Unbound fluorescein is a small hydrophilic molecule, used as a permeability marker,[44] and thus is likely to be diffusing too rapidly through the highly permeable endothelial monolayer into the surfactant to preferentially outline microvessels. A recent small study using only a fixed dose of IV fluorescein has suggested that there may be subtle differences in the dark bubbles in health and disease, though this was not our finding.[18] Nausea and wretching were induced by the fluorescein in one patient, but this is well recognised in gastrointestinal pCLE.[45] Additional information for acinar pCLE imaging may be gleaned in the future by using topical contrast agents such as cresyl violet and methylene blue which penetrate the cell membrane; these have been briefly described in the upper airways[17] and peripherally.[27]

This study has demonstrated that pCLE is quick and safe for patients with PLDs. Minor self-limiting bleeding in 3 patients was no more significant than that sometimes observed in other bronchoscopic procedures; even for a patient with a slight coagulation abnormality. Whilst the probe can cause pleuritic pain, no pneumothoraces were identified during the study. However, damage to the

delicate pulmonary acinus cannot be excluded. For example, the terminal and respiratory bronchioles are substantially narrower than the 1.4 mm diameter probe.[46] Whilst grossly magnified, free ended swaying septal walls were observed in 28 BPSs. Sometimes, this may be the product of lung disease, (more were observed in the emphysematous BPSs) but the probe was shown to be the likely culprit in several videos where the traumatic tearing of vessels and delicate septal walls was observed in real time. Whether this has any minor clinical significance remains to be established, but the areas affected are tiny, and the trauma should still be less than for TBB.

Conclusion

An *in vivo* instrument such as pCLE has theoretical advantages over conventional histology. Within the acinus, we observed both mobile cells and cyclical movement related to respiration. There were no significant complications and there was no delay or alteration (from histological preparation) to the structure observed. However, with the exception of emphysema, there is significant diagnostic information lost with pCLE as compared with histopathology. Whilst this study provides a basis to develop pCLE for PLD imaging, further work is needed before it can be used to either provide accurate diagnosis without tissue biopsy, or simply indicate the optimal subsegmental bronchus for the forceps to enhance the yield of TBB. In addition to the use of intracellular contrast agents as previously mentioned, pCLE imaging of endogenous structures other than elastin may also be realised by employing combinations of confocal wavelengths to provoke simultaneous autofluorescence from multiple endogenous sources such as collagen,[47] or by combining "fluorescence lifetime imaging" with confocal endomicroscopy to add molecular contrast to images by displaying the fluorescence decay profiles.[48]

Acknowledgements

Imperial College's pCLE hardware was partially funded by its RT-ISIS grant from the EPSRC.

Conflict of interest statement

There are no conflicts of interest.

References

1. Evidence NIfC, editor. *The diagnosis and treatment of lung cancer: methods, evidence and guidance* 2005.
2. Flaherty KR, King Jr TE, Raghu G, Lynch 3rd JP, Colby TV, et al. Idiopathic interstitial pneumonia: what is the effect of a multidisciplinary approach to diagnosis? *Am J Respir Crit Care Med* 2004;**170**:904—10.
3. Zhang D, Liu Y. Surgical lung biopsies in 418 patients with suspected interstitial lung disease in China. *Intern Med* 2010; **49**:1097—102.
4. Izbicki G, Shitrit D, Yarmolovsky A, Bendayan D, Miller G, et al. Is routine chest radiography after transbronchial biopsy necessary?: a prospective study of 350 cases. *Chest* 2006;**129**:1561—4.
5. Hanson RR, Zavala DC, Rhodes ML, Keim LW, Smith JD. Transbronchial biopsy via flexible fiberoptic bronchoscope; results in 164 patients. *Am Rev Respir Dis* 1976;**114**:67—72.
6. Smyth CM, Stead RJ. Survey of flexible fibreoptic bronchoscopy in the United Kingdom. *Eur Respir J* 2002;**19**:458—63.
7. Andersen HA. Transbronchoscopic lung biopsy for diffuse pulmonary diseases. Results in 939 patients. *Chest* 1978;**73**:734—6.
8. O'Brien JD, Ettinger NA, Shevlin D, Kollef MH. Safety and yield of transbronchial biopsy in mechanically ventilated patients. *Crit Care Med* 1997;**25**:440—6.
9. Herth FJ, Becker HD, Ernst A. Aspirin does not increase bleeding complications after transbronchial biopsy. *Chest* 2002;**122**:1461—4.
10. Jimenez MF. Prospective study on video-assisted thoracoscopic surgery in the resection of pulmonary nodules: 209 cases from the Spanish video-assisted thoracic surgery study group. *Eur J Cardiothorac Surg* 2001;**19**:562—5.
11. Lam S, MacAulay C, leRiche JC, Palcic B. Detection and localization of early lung cancer by fluorescence bronchoscopy. *Cancer* 2000;**89**:2468—73.
12. Shibuya K, Hoshino H, Chiyo M, Iyoda A, Yoshida S, et al. High magnification bronchovideoscopy combined with narrow band imaging could detect capillary loops of angiogenic squamous dysplasia in heavy smokers at high risk for lung cancer. *Thorax* 2003;**58**:989.
13. Lam S, Standish B, Baldwin C, McWilliams A, leRiche J, et al. In vivo optical coherence tomography imaging of preinvasive bronchial lesions. *Clin Cancer Res* 2008;**14**:2006—11.
14. Tanaka M, Takizawa H, Satoh M, Okada Y, Yamasawa F, et al. Assessment of an ultrathin bronchoscope that allows cytodiagnosis of small airways. *Chest* 1994;**106**:1443—7.
15. Thiberville L, Moreno-Swirc S, Vercauteren T, Peltier E, Cave C, et al. In vivo imaging of the bronchial wall microstructure using fibered confocal fluorescence microscopy. *Am J Respir Crit Care Med* 2007;**175**:22—31.
16. Musani AI, Sims M, Sareli C, Russell W, McLaren WJ, et al. A pilot study of the feasibility of confocal endomicroscopy for examination of the human airway. *J Bronchology Interv Pulmonology* 2010;**17**:126—30.
17. Lane PM, Lam S, McWilliams A, Leriche JC, Anderson MW, et al. Confocal fluorescence microendoscopy of bronchial epithelium. *J Biomed Opt* 2009;**14**:024008.
18. Fuchs FS, Zirlik S, Hildner K, Frieser M, Ganslmayer M, et al. Fluorescein-aided confocal laser endomicroscopy of the lung. *Respiration* 2011;**81**:32—8.
19. Thiberville L, Salaun M, Lachkar S, Dominique S, Moreno-Swirc S, et al. Human in vivo fluorescence microimaging of the alveolar ducts and sacs during bronchoscopy. *Eur Respir J* 2009;**33**:974—85.
20. Becker V, Vercauteren T, von Weyhern CH, Prinz C, Schmid RM, et al. High-resolution miniprobe-based confocal microscopy in combination with video mosaicing (with video). *Gastrointest Endosc* 2007;**66**:1001—7.
21. Pohl H, Rosch T, Vieth M, Koch M, Becker V, et al. Miniprobe confocal laser microscopy for the detection of invisible neoplasia in patients with Barrett's oesophagus. *Gut* 2008;**57**: 1648—53.
22. Buchner AM, Shahid MW, Heckman MG, Krishna M, Ghabril M, et al. Comparison of probe-based confocal laser endomicroscopy with virtual chromoendoscopy for classification of colon polyps. *Gastroenterology* 2009;**138**:834—42.
23. Newton RC, Kemp S, Elson DS, Yang G-Z, Thomas CMR, et al. Confocal endomicroscopy in diffuse lung diseases - initial results and future directions. *Am J Respir Crit Care Med* 2010; **181**:A6620.

24. Bergin C, Müller N, Nichols D, Lillington G, Hogg J, et al. The diagnosis of emphysema. A computed tomographic-pathologic correlation. *Am review Respiratory Disease* 1986;**133**:541.
25. Prakash UB, Fontana RS. Functional classification of bronchial carinae. *Chest* 1984;**86**:770—2.
26. Newton RC, Kemp S, Yang GZ, Darzi A, Sheppard M, et al. Tracheobronchial amyloidosis and confocal endomicroscopy. *Respiration* 2011;**82**:209—11.
27. Thiberville L, Salaun M, Lachkar S, Moreno-Swirc S, Bourg-Heckly G. In-vivo confocal endomicroscopy of peripheral lung nodules using 488nm/660nm induced fluorescence and topical methylene blue. *Eur Respir Soc Berlin* 2008:263s—4s.
28. Lesur O, Thiberville L. Vers une évaluation in vivo, en temps réel, de la réparation pulmonaire dans le SDRA: une place pour la micro-imagerie de fluorescence par laser confocal? *Réanimation* 2009;**18**:111—3.
29. Leslie KO, Gruden JF, Parish JM, Scholand MB. Transbronchial biopsy interpretation in the patient with diffuse parenchymal lung disease. *Arch Pathol Lab Med* 2007;**131**:407—23.
30. Raghu G, Nicholson AG, Lynch D. The classification, natural history and radiological/histological appearance of idiopathic pulmonary fibrosis and the other idiopathic interstitial pneumonias. *Eur Respir Rev* 2008;**17**:108—15.
31. Honda T, Ota H, Arai K, Hayama M, Fujimoto K, et al. Three-dimensional analysis of alveolar structure in usual interstitial pneumonia. *Virchows Arch* 2002;**441**:47—52.
32. Mariani TJ, Crouch E, Roby JD, Starcher B, Pierce RA. Increased elastin production in experimental granulomatous lung disease. *Am J Pathol* 1995;**147**:988—1000.
33. Deslee G, Woods JC, Moore CM, Liu L, Conradi SH, et al. Elastin expression in very severe human COPD. *Eur Respir J* 2009;**34**:324—31.
34. Hoff CR, Perkins DR, Davidson JM. Elastin gene expression is upregulated during pulmonary fibrosis. *Connect Tissue Res* 1999;**40**:145—53.
35. Black PN, Ching PS, Beaumont B, Ranasinghe S, Taylor G, et al. Changes in elastic fibres in the small airways and alveoli in COPD. *Eur Respir J* 2008;**31**:998—1004.
36. Rabe KF, Hurd S, Anzueto A, Barnes PJ, Buist SA, et al. Global strategy for the diagnosis, management, and prevention of chronic obstructive pulmonary disease: GOLD executive summary. *Am J Respir Crit Care Med* 2007;**176**:532—55.
37. Toshima M, Ohtani Y, Ohtani O. Three-dimensional architecture of elastin and collagen fiber networks in the human and rat lung. *Arch Histol Cytol* 2004;**67**:31—40.
38. Liebow AA. Pulmonary emphysema with special reference to vascular changes. *Am Review Respir Disease* 1959;**80**:67—93.
39. Wiebe BM, Laursen H. Lung morphometry by unbiased methods in emphysema: bronchial and blood vessel volume, alveolar surface area and capillary length. *APMIS* 1998;**106**:651—6.
40. Peinado VI, Pizarro S, Barbera JA. Pulmonary vascular involvement in COPD. *Chest* 2008;**134**:808—14.
41. Skold CM, Hed J, Eklund A. Smoking cessation rapidly reduces cell recovery in bronchoalveolar lavage fluid, while alveolar macrophage fluorescence remains high. *Chest* 1992;**101**:989—95.
42. Ghio AJ, Sangani RG, Brighton LE, Carson JL. MRT letter: autofluorescence by human alveolar macrophages after in vitro exposure to air pollution particles. *Microsc Res Tech* 2009.
43. Liu H, Li YQ, Yu T, Zhao YA, Zhang JP, et al. Confocal endomicroscopy for in vivo detection of microvascular architecture in normal and malignant lesions of upper gastrointestinal tract. *J Gastroenterol Hepatol* 2008;**23**:56—61.
44. Hermanns MI, Unger RE, Kehe K, Peters K, Kirkpatrick CJ. Lung epithelial cell lines in coculture with human pulmonary microvascular endothelial cells: development of an alveolocapillary barrier in vitro. *Lab Invest* 2004;**84**:736—52.
45. Wallace MB, Meining A, Canto MI, Fockens P, Miehlke S, et al. The safety of intravenous fluorescein for confocal laser endomicroscopy in the gastrointestinal tract. *Aliment Pharmacol Ther* 2010;**31**:548—52.
46. Horsfield K, Cumming G. Morphology of the bronchial tree in man. *J Appl Physiol* 1968;**24**:373—83.
47. Jean F, Bourg-Heckly G, Viellerobe B. Fibered confocal spectroscopy and multicolor imaging system for in vivo fluorescence analysis. *Opt Express* 2007;**15**:4008—17.
48. Kennedy GT, Manning HB, Elson DS, Neil MA, Stamp GW, et al. A fluorescence lifetime imaging scanning confocal endomicroscope. *J Biophotonics* 2010;**3**:103—7.